

A Novel Solid-State Electrochemiluminescence Sensor Based on poly(3-amino-4 hydroxybenzenesulfonic acid) /Ru(bpy)₃²⁺ Modified Electrode for Determination of Malachite Green

Qiu-feng Lan¹, Wen-chang Wang², Xiao-hui Chen³, Zhi-dong Chen^{4,*}

¹ School of Petrochemical Engineering, Changzhou University, China.

² School of Petrochemical Engineering, Changzhou University, China

³ School of Chemistry and Material Engineering, Changzhou Vocational Institute of Engineering, China.

⁴ School of Petrochemical Engineering, Changzhou University, China.

*E-mail: zdchen@cczu.edu.cn

Received: 12 April 2017 / Accepted: 9 May 2017 / Published: 12 June 2017

The poly(3-amino-4-hydroxybenzenesulfonic acid)/Ru(bpy)₃²⁺ modified glassy carbon electrode (PAHBS/Ru(bpy)₃²⁺/GCE) is a novel solid-state electrochemiluminescence (ECL) sensor. It was prepared by electropolymerization of 3-amino-4-hydroxybenzenesulfonic acid (AHBS) followed by soaking into Ru(bpy)₃²⁺ solution. Ru(bpy)₃²⁺ was entrapped on the electrode via the electrostatic interactions between sulfonic acid groups and Ru(bpy)₃²⁺ cation. The morphology and composition of the modified electrodes were analysed using scanning electron microscope and energy-dispersed spectrum. Cyclic voltammetry and electrochemical impedance spectroscopy were used to compare the electrochemical behavior of the electrodes before and after modification. Under the optimal conditions, the ECL intensity of the quenching value (Δ ECL) versus the logarithm of the concentration of malachite green (MG) was linear over a concentration range from 5.0×10^{-8} to 1.0×10^{-5} mol L⁻¹ ($r = 0.9931$) and the limit of detection (LOD) was 2.5×10^{-8} mol L⁻¹. This method has been successfully applied to the determination of MG in pond water.

Keywords: 3-amino-4-hydroxybenzenesulfonic acid, electrochemiluminescence, Ru(bpy)₃²⁺, malachite green, sensor

1. INTRODUCTION

Malachite green (MG) is a cationic dye, which belongs to triphenylmethane dye [1-4]. It is a therapeutic agent in aquaculture industry and has underlying risks of carcinogenicity, mutagenicity and teratogenicity [5-7]. Methods have been developed to detect MG, such as spectrophotometry [8-9],

Raman spectrometry [10], mass spectrometry [11] and high performance liquid chromatography (HPLC) [12] etc. These methods are expensive and time-consuming.

Comparing to the traditional methods, the electrochemiluminescence (ECL) offers high sensitivity, good reproducibility, low detection limit (LOD), low background noise and fast detection [13-18]. Besides, the equipment for ECL is rather simple that reduces the cost. Several electrodes have been developed for ECL detection of MG, i.e. glass carbon electrode (GCE) in luminol solution [19], Au electrode in the $\text{Ru}(\text{bpy})_3^{2+}$ solution [20]. These electrodes are effective, but consume quite a bit expensive luminescence dosage. Compared with liquid-state ECL sensor, the solid-state $\text{Ru}(\text{bpy})_3^{2+}$ ECL sensor can reduce the use of the luminescence dosage and improve of the ECL signal of $\text{Ru}(\text{bpy})_3^{2+}$ [21-23]. Therefore, it is important to develop a solid-state $\text{Ru}(\text{bpy})_3^{2+}$ ECL sensor.

The solid-state $\text{Ru}(\text{bpy})_3^{2+}$ ECL sensor can be prepared by immobilization of $\text{Ru}(\text{bpy})_3^{2+}$ on conducting polymers films, i.e. poly(p-styrenesulfonate) [24], poly(2-methoxyaniline-5-sulfonic acid) [25] and poly(4-amino-3-hydroxy-naphthalene sulfonic acid) [26], via electrostatic interaction with sulfonate groups. So far, the PAHBS film has not been applied to immobilize $\text{Ru}(\text{bpy})_3^{2+}$. The PAHBS film has (-SO₃H), (-OH) and (-NH₂) active functional groups. The active anionic functional group in the polymer structure such as the sulfonate may give rise to an obvious interactions with Ru(II) metal centers. Thus, the conjugated polymer backbone can provide direct coordination of the Ru(II) metal centers by electronic interactions. The PAHBS film is extraordinary materials to immobilize $\text{Ru}(\text{bpy})_3^{2+}$ on the surface electrode.

In this paper, a new approach was developed for constructing a ECL sensor via electrochemical polymerization 3-amino-4-hydroxybenzenesulfonic acid (AHBS) monomer at glassy carbon electrode (GCE) and then soaking in $\text{Ru}(\text{bpy})_3^{2+}$ solution to prepare PAHBS/ $\text{Ru}(\text{bpy})_3^{2+}$ /GCE. This method can reduce the consumption of expensive reagent and amplify the ECL signal to provide a fast detection and low cost sensor for the determination of MG. It provides a novel solid-state ECL sensor for determination of MG.

2. EXPERIMENTAL

2.1. Reagents

Malachite green (MG, 95%), 3-amino-4-hydroxybenzenesulfonic acid (AHBS, 98%), Tris(2,2'-bipyridyl) ruthenium(II) chloride hexahydrate ($\text{Ru}(\text{bpy})_3\text{Cl}_2 \cdot 6\text{H}_2\text{O}$, 98%), potassium hexacyanoferrate(II) ($\text{K}_4[\text{Fe}(\text{CN})_6] \cdot 3\text{H}_2\text{O}$, 99.5%), potassium hexacyanoferrate(III) ($\text{K}_3[\text{Fe}(\text{CN})_6]$, 99.5%), potassium chloride (KCl, 99.8%), disodium hydrogen phosphate dodecahydrate ($\text{Na}_2\text{HPO}_4 \cdot 12\text{H}_2\text{O}$, 99.0%), sodium dihydrogen phosphate ($\text{NaH}_2\text{PO}_4 \cdot 2\text{H}_2\text{O}$, 99.0%), sodium hydroxide (NaOH, 96.0%), phosphoric acid (H_3PO_4 , 85.0%) and ethanol ($\text{CH}_3\text{CH}_2\text{OH}$, 99.7%) were purchased from Aladdin (Shanghai, China). Double distilled water was used in all experimental process.

2.2. Apparatus

Electrochemical polymerization and electrochemical impedance spectroscopy (EIS) were conducted with a CHI 660D Electrochemical Workstation (Shanghai CH instrument Co., Ltd., China). ECL measurement was performed on MPI-B multifunctional ECL system (Xi'an Remex Analyse Instrument Co., Ltd., China). Scanning electron micrographs of the electrode surfaces were obtained using a JEOL (JSM-6360LA, Japan) scanning electron microscope (SEM). The energy-dispersed spectrum (EDS) analysis was performed using a JEOL (JSM-6360LA, Japan) system.

2.3. Preparation of $\text{Ru}(\text{bpy})_3^{2+}/\text{GCE}$

Prior to surface modification, the glassy carbon electrode (GCE, $\phi = 3 \text{ mm}$) was first polished with $0.50 \mu\text{m}$, $0.30 \mu\text{m}$ and $0.05 \mu\text{m}$ alumina powder respectively. After polishing, the electrode was sonicated in ethanol and water, respectively, and then was dried in a stream of air. The GCE was soaked in $15 \text{ mL } 1.0 \times 10^{-4} \text{ mol L}^{-1} \text{ Ru}(\text{bpy})_3^{2+}$ solution for 30 min to prepare $\text{Ru}(\text{bpy})_3^{2+}$ modified glassy carbon electrode ($\text{Ru}(\text{bpy})_3^{2+}/\text{GCE}$).

2.4. Preparation of $\text{PAHBS}/\text{Ru}(\text{bpy})_3^{2+}/\text{GCE}$

The PAHBS modified glassy carbon electrode (PAHBS/GCE) was prepared in a solution containing 0.1 mol L^{-1} phosphate buffer solution (PBS, pH 7.5) as supporting electrolyte and $4.0 \times 10^{-3} \text{ mol L}^{-1}$ AHBS monomer by cycling the electrode potential between -1.5 V and $+2.0 \text{ V}$ for 20 cycles with a scan rate of 0.1 V s^{-1} . The PAHBS/GCE was then soaked in $15 \text{ mL } 1.0 \times 10^{-4} \text{ mol L}^{-1} \text{ Ru}(\text{bpy})_3^{2+}$ solution for 30 min. The electrode was washed carefully by the double distilled water, and dried at room temperature to prepare $\text{PAHBS}/\text{Ru}(\text{bpy})_3^{2+}/\text{GCE}$. A three-electrode system was used for ECL measurement. The working electrode was $\text{PAHBS}/\text{Ru}(\text{bpy})_3^{2+}/\text{GCE}$; the reference electrode was an Ag/AgCl electrode and a platinum disk ($\phi = 3 \text{ mm}$) was used as the auxiliary electrode. The steps and ECL measurement process for the determination of MG are presented in Fig. 1.

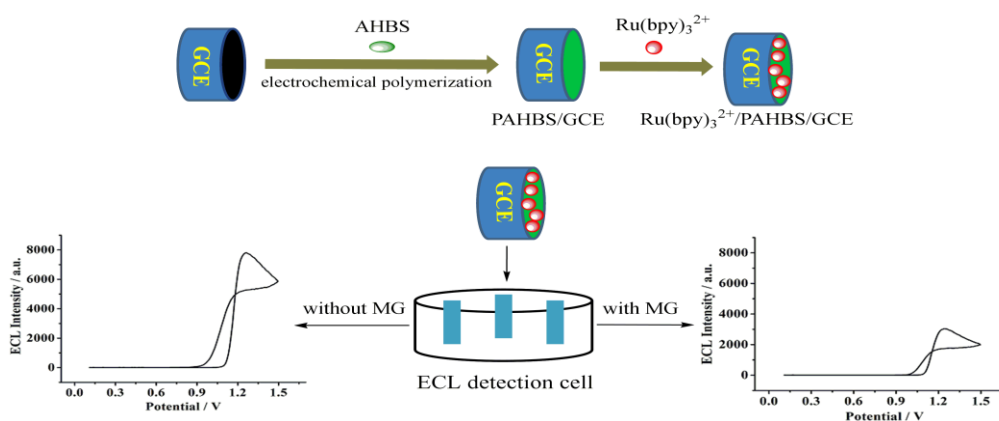


Figure 1. Process of preparing modified glassy carbon electrode (top) and ECL measurement (bottom).

3. RESULTS AND DISCUSSION

3.1. Characterization of Electrode

Fig. 2 shows the SEM images of glassy carbon electrode (GCE), poly(3-amino-4-hydroxybenzenesulfonic acid) modified glassy carbon electrode (PAHBS/GCE) and poly(3-amino-4-hydroxybenzenesulfonic acid)/Ru(bpy)₃²⁺ modified glassy carbon electrode (PAHBS/Ru(bpy)₃²⁺/GCE). GCE, PAHBS/GCE and PAHBS/Ru(bpy)₃²⁺/GCE have different surface morphologies. The GCE electrode is very smooth (Fig. 2A). Fig. 2B shows that the surface of PAHBS/GCE has a layered structure which provides site for the adsorption of Ru(bpy)₃²⁺. After immobilization of Ru(bpy)₃²⁺ on PAHBS/GCE, the layered structure is less pronounced (Fig. 2C). In order to demonstrate that the Ru(bpy)₃²⁺ have been successfully immobilized on PAHBS/GCE, the PAHBS/Ru(bpy)₃²⁺/GCE is further analysed by the energy-dispersed spectrum (EDS) (Fig. 2D). The peaks of C, O, S and Ru elements are observed (Pt peaks were originated from the sputtered Pt conducting layer), indicating the Ru(bpy)₃²⁺ is immobilized on PAHBS/GCE surface [27-28].

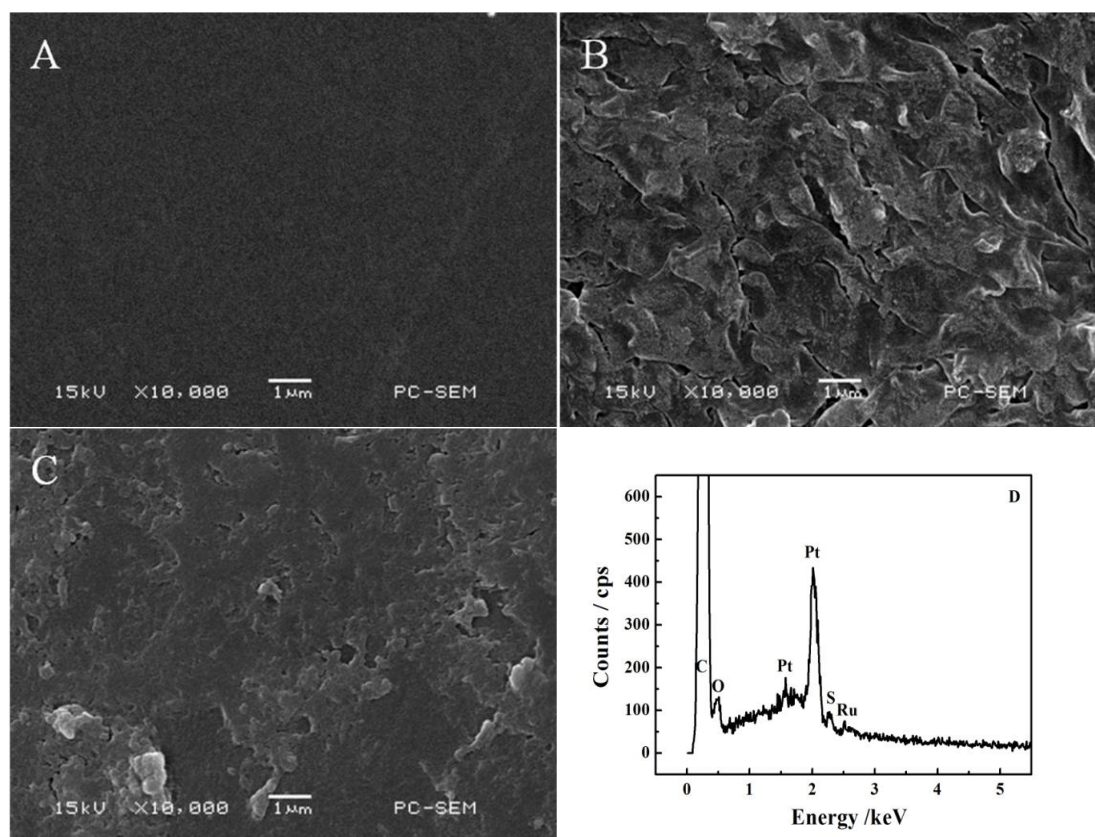


Figure 2. SEM images of GCE (A), and PAHBS/GCE (B) and PAHBS/Ru(bpy)₃²⁺/GCE (C). EDS spectra of the PAHBS/Ru(bpy)₃²⁺/GCE (D)

3.2. Electrochemical Characterization

Fig. 3A shows the cyclic voltammograms (CVs) of bare GCE (a), PAHBS/GCE (b) and PAHBS/Ru(bpy)₃²⁺/GCE (c) between 0.2 V and 0.6 V in 5.0×10^{-3} mol L⁻¹ Fe(CN)₆^{3-/4-} solution

containing 0.1 mol L^{-1} KCl as supporting electrolyte. A pair of well-defined redox peaks appears at the bare GCE (curve a), which is attributed to the redox between $\text{Fe}(\text{CN})_6^{3-}$ and $\text{Fe}(\text{CN})_6^{4-}$. Fig. 3A (curve b) shows that the peak current decreased when PAHBS was modified on the GCE indicating that PAHBS was successfully immobilized by electrochemical polymerization. The peak currents decreased at the PAHBS/GCE due to the low electrical conductivity of the PAHBS film [29]. An increase in current was found (Fig. 3A (curve c)) when $\text{Ru}(\text{bpy})_3^{2+}$ was modified on the PAHBS/GCE electrode due to the electrostatic interactions between $\text{Fe}(\text{CN})_6^{3-/4-}$ and $\text{Ru}(\text{bpy})_3^{2+}$ which accelerate the electron transfer of $\text{Fe}(\text{CN})_6^{3-/4-}$ onto the electrode surface [30]. A peak-to-peak potential separation (ΔE_p) of GCE (curve a), PAHBS/GCE (curve b) and PAHBS/ $\text{Ru}(\text{bpy})_3^{2+}$ /GCE (curve c) are 108 mV, 161 mV and 131 mV, respectively. It was reported that the value of ΔE_p is related to the electron transfer coefficient [31], and a low ΔE_p suggests a fast for a single electron electrochemical reaction [32-33]. Electrochemical impedance spectroscopy techniques was further used to analyse modified electrodes. As can be seen from Fig. 3B, electron-transfer resistance of GCE is 82.96Ω (curve a), indicating the electroactive ion $\text{Fe}(\text{CN})_6^{3-}$ and $\text{Fe}(\text{CN})_6^{4-}$ are transported fast on the GCE interface. The electron-transfer resistance increased to 359.1Ω (curve b) with the introduction of PAHBS film due to its low electrical conductivity. However, the PAHBS/ $\text{Ru}(\text{bpy})_3^{2+}$ /GCE exhibits a moderate electron-transfer resistance of 237.1Ω (curve c) which could be due to the electrostatic interaction of positively charged ruthenium complex immobilized in the film and the negatively charged ferricyanide allowing more electrochemical probes access the electrode surface for electron transfer reaction [34].

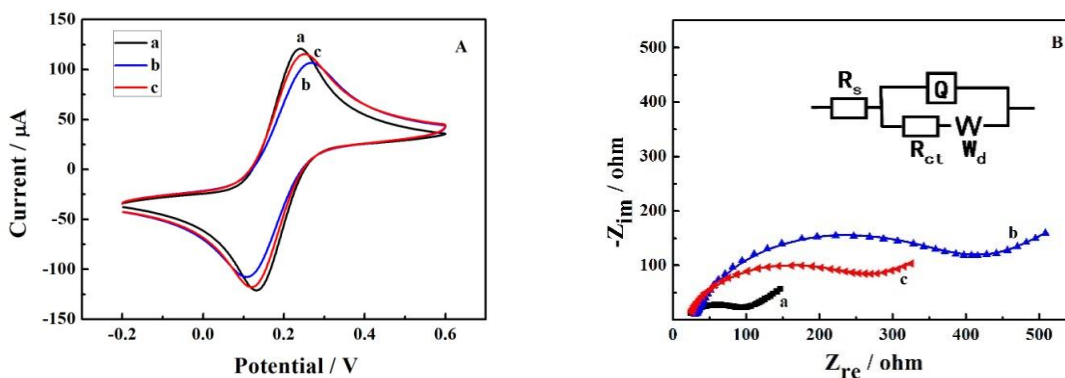


Figure 3. (A) Cyclic voltammograms of bare GCE (a), PAHBS/GCE (b) and PAHBS/ $\text{Ru}(\text{bpy})_3^{2+}$ /GCE (c) in $5.0 \times 10^{-3} \text{ mol L}^{-1}$ $\text{Fe}(\text{CN})_6^{3-/4-}$ solution containing 0.1 mol L^{-1} KCl; The scan rate was $5.0 \times 10^{-2} \text{ V s}^{-1}$. (B) EIS represented by the Nyquist diagram of bare GCE (a), PAHBS/GCE (b) and PAHBS/ $\text{Ru}(\text{bpy})_3^{2+}$ /GCE (c) in the presence of $5.0 \times 10^{-3} \text{ mol L}^{-1}$ $[\text{Fe}(\text{CN})_6]^{3-/4-}$ in 0.1 mol L^{-1} KCl. Inset: equivalent circuit (top).

3.3. The ECL Behavior of MG on Different Modified Electrode

The ECL behaviors of different modified electrodes have been studied. Fig. 4 shows the ECL-potential curve of PAHBS/ $\text{Ru}(\text{bpy})_3^{2+}$ /GCE in the 0.1 mol L^{-1} PBS (pH 10.0) solution either without (curve a) or with (curve b) $5.0 \times 10^{-7} \text{ mol L}^{-1}$ MG. The potential region was from 0.1 V to 1.5 V and the scan rate was 0.1 V s^{-1} . A giant quenched ECL value (ΔECL , 2074) was observed which is

consistent with the $\text{Ru}(\text{bpy})_3^{2+}$ -MG reaction system reported by Liu et al. [20]; The ΔECL of $\text{Ru}(\text{bpy})_3^{2+}/\text{GCE}$ in the 0.1 mol L^{-1} PBS (pH 10.0) without (curve c) and with (curve d) $5.0 \times 10^{-7} \text{ mol L}^{-1}$ MG is 109. The ΔECL increased from 109 to 2074 as PAHBS was modified on the electrode indicating that PAHBS film can amplify the ECL signal.

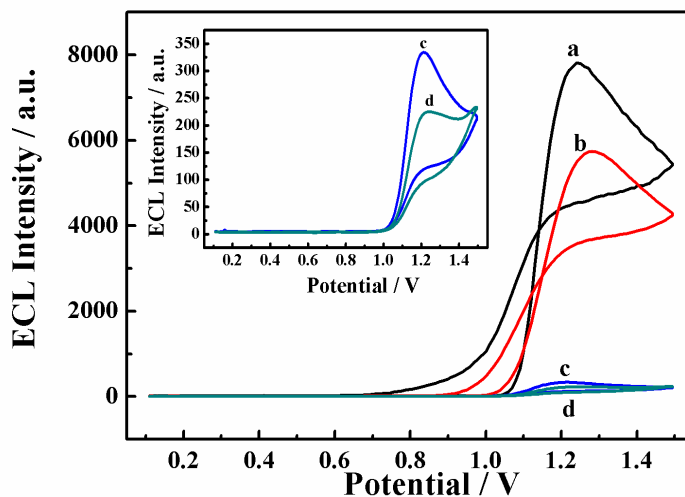


Figure 4. ECL-potential curves for PAHBS/ $\text{Ru}(\text{bpy})_3^{2+}/\text{GCE}$ in 0.1 mol L^{-1} PBS (pH 10.0) without (a) and with (b) $5.0 \times 10^{-7} \text{ mol L}^{-1}$ MG; ECL-potential curve for $\text{Ru}(\text{bpy})_3^{2+}/\text{GCE}$ in 0.1 mol L^{-1} PBS (pH 10.0) without (c) or with (d) $5.0 \times 10^{-7} \text{ mol L}^{-1}$ MG. Inset: magnified ECL-potential curve for $\text{Ru}(\text{bpy})_3^{2+}/\text{GCE}$ in 0.1 mol L^{-1} PBS (pH 10.0) without (c) or with (d) $5.0 \times 10^{-7} \text{ mol L}^{-1}$ MG. The scan rate was 0.1 Vs^{-1} .

3.4. Optimization

The ΔECL was correlated with several factors, such as the thickness and uniformity of PAHBS layer which depends on polymerization conditions (i.e. the concentration of AHBS), the amount of $\text{Ru}(\text{bpy})_3^{2+}$ adsorbed on the electrode which is a function of absorbing time, and the testing conditions (the pH of PBS and scan rate). In order to obtain a higher sensitivity of ECL, all these factors were optimized.

The concentration of AHBS affects the coverage and the thickness of PAHBS on the electrode surface. Fig. 5A shows effect of concentration of AHBS on ΔECL . At lower concentrations ($< 4.0 \times 10^{-3} \text{ mol L}^{-1}$), the ΔECL increases with the concentration of AHBS. This is because at low concentration, the electrode was not fully covered by the PAHBS. When the concentration of AHBS was $4.0 \times 10^{-3} \text{ mol L}^{-1}$, the ΔECL reached the peak value. When the concentration of AHBS was more than $4.0 \times 10^{-3} \text{ mol L}^{-1}$, thicker films were obtained leading to the low rate of electron transfer in the PAHBS film.

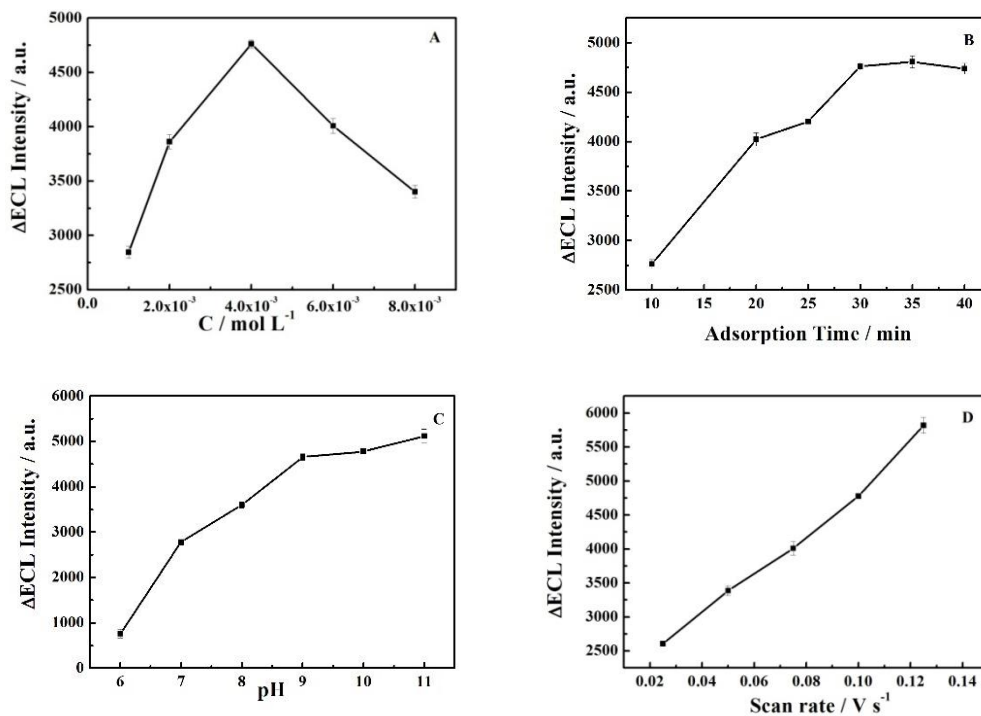


Figure 5. (A) Effect of the concentration of AHBS on ΔECL , (B) Effect of the adsorption time on ΔECL in the presence of $1.0 \times 10^{-4} \text{ mol L}^{-1} \text{ Ru}(\text{bpy})_3^{2+}$ solution, (C) Effect of pH on ΔECL and (D) Effect of scan rate on ΔECL .

The dipping time of PAHBS/GCE in $\text{Ru}(\text{bpy})_3^{2+}$ solution determines the amount of $\text{Ru}(\text{bpy})_3^{2+}$ absorbing on the electrode which affects the ECL intensity [35]. A series of adsorption time from 10 min to 40 min was studied in 15 mL $1.0 \times 10^{-4} \text{ mol L}^{-1} \text{ Ru}(\text{bpy})_3^{2+}$ solution (Fig. 5B). The ΔECL increased as the adsorption time increased from 10 min to 30 min. After 30 min, the ΔECL reached to a plateau.

The ECL process depends on the pH of the testing solution [36]. As shown Fig. 5C when the pH of PBS increased from 6.0 to 10.0, the ΔECL increased due to $\text{Ru}(\text{bpy})_3^{2+}$ have good luminescence properties under the alkaline condition [21]. When the pH of PBS was more than 10.0, the ΔECL became unstable. Thus, pH of 10.0 was selected as optimal condition.

The ECL efficiency depends on the rate of generation/annihilation of the excited state $\text{Ru}(\text{bpy})_3^{2+*}$ [20]. The testing scan rate also affects the ECL intensity of $\text{Ru}(\text{bpy})_3^{2+}$ as shown in Fig. 5D. The ΔECL increased as the scan rate increased from 0.025 V s^{-1} to 0.125 V s^{-1} . At 0.1 V s^{-1} , the ΔECL had a stable reproducibility. Therefore, the scan rate of 0.1 V s^{-1} was chosen as the optimal condition.

Considering the sensitivity of the ECL sensor, $4.0 \times 10^{-3} \text{ mol L}^{-1}$ concentration of AHBS was used to prepare PAHBS film. PAHBS/GCE was immersed in $\text{Ru}(\text{bpy})_3^{2+}$ solution for 30 min to form $\text{Ru}(\text{bpy})_3^{2+}$ modified electrode. pH of 10.0 and 0.1 V s^{-1} of scan rate were used in the following experiments.

3.5. Detection of MG with the Proposed Sensor

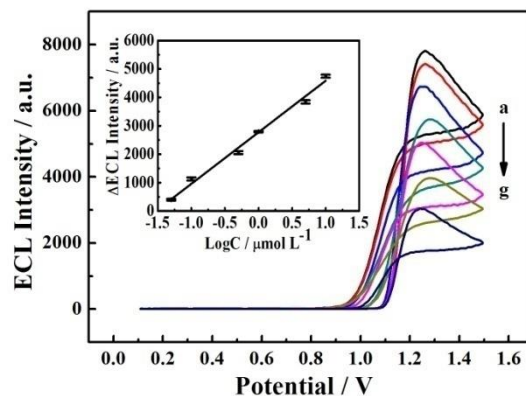


Figure 6. ECL-potential curves of the PAHBS/Ru(bpy)₃²⁺/GCE with different concentrations of MG. Concentration of MG (μmol L⁻¹): (a) 0, (b) 0.05, (c) 0.1, (d) 0.5, (e) 1.0, (f) 5.0, (g) 10. Inset: the linear relationship between the ΔECL and the logarithmic concentration of MG.

Table 1. Comparison between the ECL assay and other reported methods for the detection of MG.

Methods	Linear range μmol/L ⁻¹	LOD μmol/L ⁻¹	Ref.
spectrophotometry	0.100-20.0	0.059	[8]
	0.129-1.294	0.0088	[9]
Raman spectroscopy	0.108-10.787	-	[10]
mass spectrometry	0.0216-21.570	0.0082	[11]
HPLC	10.787-215.70	0.00123	[12]
liquid-state ECL	0.010-10.0	0.010	[20]
solid-state ECL	0.050-10.0	0.025	This work

Under the optimal conditions, different concentrations of MG was added. The ΔECL was found in good linear relationship with the logarithm of the concentration from 5.0×10^{-8} to 1.0×10^{-5} mol L⁻¹ (Fig. 6), and the detection limit (LOD) was 2.5×10^{-8} mol L⁻¹. The regression equation was $\Delta\text{ECL} = 2779.42 + 1786.13\log C$ (μmol L⁻¹), and the correlation coefficient was 0.9931. The relative standard deviations (RSDs) were less than 5.0%. The proposed sensor was compared with other methods detecting MG and the results are reported in Table 1. The proposed sensor exhibits a wide linear range. Comparing to most of the reported methods, the proposed sensor is much simpler and cost efficient.

3.6. Interference Study

The pond water have several underlying interferences for MG detection, such as K_2SO_4 , Na_2SO_4 , $NaCl$, KCl , KNO_3 , $NaNO_3$, $NaCO_3$, $MgSO_4$ NH_4Cl and glucose. Those underlying interferences were investigated. Therefore, not much interference could be observed when the acceptable molar concentration ratios for interference were 1000 folds for K_2SO_4 , Na_2SO_4 , $NaCl$, KCl , KNO_3 , $NaNO_3$ and $NaCO_3$, 100 folds for $MgSO_4$, 250 folds for NH_4Cl and glucose. Most of the compounds had no significant effect on the detection of $1.0 \times 10^{-5} \text{ mol L}^{-1}$ MG, leading to a relative error of less than 5.0%. The ECL solid-state sensor displayed favorable selectivity in detecting MG.

3.7. Analytical Application

In order to study the developed ECL sensor's capability of detecting MG in pond water, MG was added into pond water samples. Pond water from three different locations were investigated. Before addition of MG, the pond water was tested by means of spectrophotometry [9]. It was proven that no MG was found in pond water. The analytical results are shown in Table 2. It is obvious that the recoverys were 98.00-103.00% at a PAHBS/Ru(bpy) $_3^{2+}$ /GCE. The RSDs were less than 5.0%. This indicates that the PAHBS/Ru(bpy) $_3^{2+}$ /GCE sensor can be sucessfully applid to the determination of MG concentration in pond water.

Table 2. Determination of MG in a pond water sample.

Pond water	Added ($\mu\text{mol L}^{-1}$)	Detected ($\mu\text{mol L}^{-1}$)	Average ($\mu\text{mol L}^{-1}$)	Recovery (%)	RSD (%)
		0.97			
1	1.00	1.01	0.99	99.67	2.32
		1.01			
		0.97			
2	1.00	1.03	0.98	98.00	4.68
		0.94			
		1.05			
3	1.00	1.03	1.03	103.00	1.94
		1.01			

1, 2 and 3 were three different locations of the pond water.

4. CONCLUSIONS

In this paper, PAHBS/Ru(bpy) $_3^{2+}$ /GCE was successfully prepared, and was used for determination of MG. Under the optimal conditions, the PAHBS/Ru(bpy) $_3^{2+}$ /GCE sensor exhibited a

high sensitivity and a low detection limit for MG and could be applied to the detection of MG in fish pond water samples.

ACKNOWLEDGEMENTS

The authors are grateful to the National Natural Science Foundation of China (no. 21175016) for financial support of this work.

References

1. X. Hu, K. Jiao, W. Sun and J. Y. You, *Electroanalysis*, 18 (2006) 613-620.
2. J. Alexander, L. Barregård and M. Bignami, *Efsa Journal*, 14 (2016) 4530-4610.
3. C. Cha, D. Doerge and C. Cerniglia, *Appl Environ Microbiol.* 67 (2001) 4358-4360.
4. A. Franca, L. Oliveira and A. Nunes, *Clean-Soil, Air, Water*, 38 (2010) 843-849.
5. S. Liang, Z. Jia, W. Zhang, W. Wang and L. Zhang, *Materials and Design*, 119 (2017) 244-253.
6. L. Wu, Z. Lin, H. Zhong, X. Chen and Z. Huang, *Sensors and Actuators B*, 239 (2017) 69-75.
7. T. Khan, R. Rahman and E. Khan, *Model. Earth Syst. Environ.*, 3 (2017) 1-14.
8. L. Wu, Z. Lin, H. Zhong, X. Chen and Z. Huang, *Sensors and Actuators B*, 239 (2017) 69-75.
9. E. Ghasemi and M. Kaykhahi, *Spectrochim Acta Part A*, 164 (2016) 93-97.
10. Y. Zhang, Y. Huang, F. Zhai, R. Du, Y. Liu and K. Lai, *Food Chem.*, 135 (2012) 845-850.
11. X. Fang, S. Yang, K. Chingini, L. Zhu, X. Zhang, Z. Zhou and Z. Zhao, *Int. J. Environ. Res. Public Health*, 13 (2016) 1-7.
12. Z. Lin, D. Wang, H. Zhang, L. Li, Z. Huang, J. Shen and Y. Lin, *Sep. Sci. Technol.*, 51 (2016) 1-21.
13. Y. Gao, T. Wang and F. Liu, *Electroanalysis*, 28 (2016) 1-8.
14. F. Zhou, H. Hai, Y. Yuan and J. Li, *Electroanalysis*, 29 (2017) 1-8.
15. J. Wang, Y. Xu, M. Liu, F. Niu and J. Liu, *Electroanalysis*, 28 (2016) 936-939.
16. L. Wang, D. Luo, D. Qin, D. Shan and X. Lu, *Anal. Methods*, 7 (2014) 1395-1400.
17. M. Hosseini, M. Pur, P. Norouzi, M. Moghaddam, F. Ganjali, M. Reza and J. Shamsi, *Anal. Methods*, 7 (2015) 1936-1942.
18. G. Yan, X. He, K. Wang, Y. Wang, J. Liu, L. Jian and Y. Mao, *Chin. Chem. Lett.*, 25 (2014) 1520-1524.
19. Z. Guo, P. Gai, T. Hao, J. Duan and S. Wang, *J Agric Food Chem.*, 59 (2011) 5257-5262.
20. F. Liu, X. Yang, Y. Zhao and S. Sun, *Anal. Methods*, 5 (2013) 660-665.
21. Z. Liu, F. Zhang, L. Cui, K. Wang and H. Zhan, *Anal. Methods*, 9 (2017) 1011-1017.
22. A. Zhang, C. Miao, H. Shi, H. Xiang, C. Huang and N. Jia, *Sensors and Actuators B*, 222 (2016) 433-439.
23. M. Hosseini, M. Moghaddam, F. Faridbod, P. Norouzi, M. Pur and M. Ganjali, *RSC Adv.*, 5 (2015) 64669-64674.
24. J. Li, Y. H. Xu, H. Wei, T. Huo and E. Wang, *Anal. Chem.*, 79 (2007) 5439-5443.
25. L. Dennany, P. Innis, G. Wallace and R. Forster, *J. Phys. Chem. B*, 112 (2008) 12907-12912.
26. M. Al-Hinaai, E. Khudaish, S. Al-Harthy and F. Suliman, *Electrochim Acta*, 176 (2015) 179-187.
27. Y. Li, H. Zhu and X. Yang, *Talanta*, 80 (2009) 870-874.
28. X. Sun, Y. Du, S. Dong and E. Wang, *Anal Chem.*, 77 (2005) 8166-8169.
29. Q. Xiao, S. Lu, C. Huang, W. Su and S. Huang, *Sensors*, 16 (2016) 1874-1889.
30. X. Yang, R. Yuan, Y. Chai, Y. Zhuo, L. Mao and S. Yuan, *Biosensors and Bioelectronics*, 25 (2010) 1851-1855.
31. R. Nicholson, *Anal. Chem.*, 37 (1965) 1351-1355.
32. N. Shang, P. Papakonstantinou, M. McMullan, M. Chu, A. Stamboulis, A. Potenza, S. Dhesi and H. Marchetto, *Adv. Funct. Mater.*, 18 (2008) 3506-3514.

33. X. Gu, Y. Tao, Y. Pan, L. Deng, L. Bao and Y. Kong, *Anal. Chem.*, 87 (2015) 948-9486.
34. J. Yan, L. Ge, X. Song, M. Yan, S. Ge and J. Yu, *Chem. Eur. J.*, 18 (2012) 4938-4945.
35. X. Fan, S. Wang, Z. Li, P. Liu, Y. Yu, L. Chang, K. Li and X. Zheng, *J. Braz. Chem. Soc.*, 28 (2017) 277-284.
36. J. Leland and M. Powell, *J Electrochem. Soc.*, 137 (1990) 3127-3131.

© 2017 The Authors. Published by ESG (www.electrochemsci.org). This article is an open access article distributed under the terms and conditions of the Creative Commons Attribution license (<http://creativecommons.org/licenses/by/4.0/>).